

1 **Resveratrol improves TNF- $\alpha$ -induced endothelial dysfunction in a co-culture model of a**  
2 **Caco-2 with an endothelial cell line**

3  
4  
5 3

6  
7 4 Isabela Maia Toaldo<sup>a,b</sup>, John Van Camp<sup>b</sup>, Gerard Bryan Gonzales<sup>b</sup>, Senem Kamiloglu<sup>b,e</sup>,  
8  
9  
10 5 Marilde T. Bordignon-Luiz<sup>a</sup>, Guy Smaghe<sup>c</sup>, Katleen Raes<sup>d</sup>, Esra Capanoglu<sup>e</sup>, Charlotte  
11  
12 6 Grootaert<sup>b\*</sup>

13  
14  
15 7

16  
17 8 <sup>a</sup>Department of Food Science and Technology, Federal University of Santa Catarina, Admar  
18  
19 9 Gonzaga 1346, 88034001 Florianópolis, Brazil

20  
21  
22 10

23  
24 11 <sup>b</sup>Department of Food Safety and Food Quality, Ghent University, Coupure Links 653, 9000  
25  
26 12 Gent, Belgium

27  
28  
29 13

30  
31 14 <sup>c</sup>Department of Crop Protection, Faculty of Bioscience Engineering, Ghent University,  
32  
33 15 Coupure Links 653, 9000 Gent, Belgium

34  
35  
36 16

37  
38 17 <sup>d</sup>Department of Industrial Biological Sciences, Faculty of Bioscience Engineering, Ghent  
39  
40 18 University, Graaf Karel de Goedelaan 5, 8500 Kortrijk, Belgium

41  
42  
43 19

44  
45  
46 20 <sup>e</sup>Department of Food Engineering, Faculty of Chemical and Metallurgical Engineering,  
47  
48 21 Istanbul Technical University, 34469 Maslak, Istanbul, Turkey.

49  
50  
51 22

52  
53 23 **\*Present address:** Dr. ir. Charlotte Grootaert, Department of Food Safety and Food Quality,  
54  
55 24 Ghent University, Coupure Links 653, 9000 Gent, Belgium. **E-mail address:**  
56  
57 25 charlotte.grootaert@ugent.be. **Tel./Fax:** +32-(0)9 264 62 08.

58  
59  
60  
61  
62  
63  
64  
65

1  
2  
3  
4  
5  
6  
7  
8  
9  
10  
11  
12  
13  
14  
15  
16  
17  
18  
19  
20  
21  
22  
23  
24  
25  
26  
27  
28  
29  
30  
31  
32  
33  
34  
35  
36  
37  
38  
39  
40  
41  
42  
43  
44  
45  
46  
47  
48  
49  
50  
51  
52  
53  
54  
55  
56  
57  
58  
59  
60  
61  
62  
63  
64  
65

26 **Abbreviations:**

27 eNOS, endothelial nitric oxide synthase; ICAM-1, intercellular adhesion molecule-1; IFN- $\gamma$ ,  
28 interferon  $\gamma$ ; IL-1, interleukin-1; IL-8, interleukin-8; KDR, tyrosine kinase receptor; NF- $\kappa$ B,  
29 transcription nuclear factor  $\kappa\beta$ ; NO, nitric oxide; ; Romo1, ROS modulator; ROS, reactive  
30 oxygen species; RSV, *trans*-resveratrol; TNF- $\alpha$ , tumor necrosis factor  $\alpha$ ; VASP, vasodilator-  
31 activated protein; VEGF, vascular endothelial growth factor.

32

33

34 **Chemical compounds studied in this article**

35 *trans*-resveratrol (PubChem CID: 445154)

36 interleukin-8 (PubChem CID: 44357137)

37

38

39

40

41

42

43

44

45

46

47

48

49

50

1  
2  
3  
4  
5  
6  
7  
8  
9  
10  
11  
12  
13  
14  
15  
16  
17  
18  
19  
20  
21  
22  
23  
24  
25  
26  
27  
28  
29  
30  
31  
32  
33  
34  
35  
36  
37  
38  
39  
40  
41  
42  
43  
44  
45  
46  
47  
48  
49  
50  
51 **Abstract**

52

53 The bioactivity of *trans*-Resveratrol (RSV), an important wine polyphenol, and of its  
54 metabolites was investigated in a more relevant setup comprising an *in vitro* co-culture cell  
55 model that combines intestinal absorption and conjugation with changes in endothelial  
56 function, which is primarily affected in cardiovascular diseases. Caco-2 and endothelial  
57 EA.hy926 cells were grown in a co-culture and Caco-2 cells were treated with RSV, in the  
58 co-culture and in two different sequential setups, for 4 h and 24 h. Transported metabolites  
59 were investigated by UPLC-MS/MS<sup>E</sup> and the effects on NO production, ROS inhibition and  
60 secretion of vascular endothelial growth factor (VEGF), interleukin-8 (IL-8) and intercellular  
61 adhesion molecule-1 (ICAM-1) were evaluated in TNF- $\alpha$ -activated and non-activated  
62 endothelial cells. RSV and four conjugated metabolites, two sulfates and two glucuronides,  
63 were identified after intestinal transport. In both co-culture and sequential systems, RSV at  
64 20  $\mu$ M strongly induced NO production. Changes in ROS and NO levels demonstrated a  
65 clear effect of crosstalk between cells in the co-culture. The secretion of proinflammatory  
66 cytokines and VEGF was largely increased by treatment with TNF- $\alpha$  (inflammatory  
67 condition). The polyphenol intervention significantly reduced the levels of VEGF, ROS, IL-8  
68 and ICAM-1, with a more pronounced effect in TNF- $\alpha$ -activated endothelial cells. In  
69 conclusion, RSV and its metabolites showed accentuated bioactivity on TNF- $\alpha$ -induced  
70 inflammation and the metabolism of endothelial cells as a biological target was not only  
71 influenced by these phenolics, but also by the communication between distinct cell lines,  
72 showing a new perspective for investigations on polyphenol intervention and its biological  
73 outcomes.

54  
55  
56  
57  
58  
59  
60  
61  
62  
63  
64  
65

74

75 **Keywords:** Cardiovascular disease; Co-culture; ICAM-1; Intestine; Nitric oxide; Resveratrol

1  
2  
3  
4  
5  
6  
7  
8  
9  
10  
11  
12  
13  
14  
15  
16  
17  
18  
19  
20  
21  
22  
23  
24  
25  
26  
27  
28  
29  
30  
31  
32  
33  
34  
35  
36  
37  
38  
39  
40  
41  
42  
43  
44  
45  
46  
47  
48  
49  
50  
51  
52  
53  
54  
55  
56  
57  
58  
59  
60  
61  
62  
63  
64  
65

76 **1 Introduction**

77

78 Cardiovascular diseases are the leading cause of death and disability in the  
79 Western world and include several pathological conditions related to dysfunction of blood  
80 vessels, including arteries, veins and capillaries [1]. Atherosclerosis is a chronic  
81 inflammatory disease characterized by the formation of atherosclerotic plaques (atheromas),  
82 caused by endothelial injury and vascular wall inflammation that trigger the accumulation of  
83 oxidized lipid molecules, infiltration of macrophages, lymphocytes and connective tissue  
84 components, and the proliferation of smooth muscle cells [1,2].

85 Oxidative stress and inflammation in endothelial cells are intimately associated with  
86 the development of atherosclerosis. Reactive oxygen species (ROS) act as potent oxidants of  
87 key biological molecules causing impairment of various cellular functions. In the  
88 endothelium, the activation of the transcription nuclear factor NF- $\kappa$ B and proinflammatory  
89 cytokines such as tumor necrosis factor  $\alpha$  (TNF- $\alpha$ ), interleukin-1 (IL-1), interleukin-8 (IL-8)  
90 and interferon  $\gamma$  (IFN)- $\gamma$  accelerates atheroma formation [3,4]. Additionally to inflammation  
91 and oxidation, the pre-events in atherosclerosis include metabolic conditions such as  
92 dyslipidemias, hypertension, diabetes and obesity, and lifestyle changes and dietary habits  
93 comprise important factors to counteract oxidative damage and inflammation [5].

94 The consumption of polyphenol-rich diets is associated with a reduced risk of chronic  
95 diseases. Grape derivatives such as wine and grape juice are highly appreciated worldwide  
96 and account for one of the most important sources of polyphenols in the human diet [6].  
97 Resveratrol (*trans*-3,5,4'-trihydroxystilbene; RSV) is an important bioactive stilbene present  
98 in grapes, red wine and berries, with health-related properties towards cardiovascular  
99 functions [7,8]. Both *in vivo* and *in vitro* research has demonstrated the potential of RSV to  
100 modulate angiogenesis [9], cell signaling [10], markers for vasorelaxation [11], expression of

1  
2  
3  
4  
5  
6  
7  
8  
9  
10  
11  
12  
13  
14  
15  
16  
17  
18  
19  
20  
21  
22  
23  
24  
25  
26  
27  
28  
29  
30  
31  
32  
33  
34  
35  
36  
37  
38  
39  
40  
41  
42  
43  
44  
45  
46  
47  
48  
49  
50  
51  
52  
53  
54  
55  
56  
57  
58  
59  
60  
61  
62  
63  
64  
65

101 inflammatory factors and adhesion molecules [12,13] and gene transcription [14]. However,  
102 RSV is strongly metabolized to glucuronated and sulfated metabolites by mostly intestine  
103 and liver [15], and especially glucuronides were shown to be less bioactive *in vitro* [16]. So  
104 far, mechanistic studies have not included the excessive RSV metabolism during intestinal  
105 absorption in their design, and crosstalk mechanisms between different cell types as an  
106 indirect result of RSV addition are often overlooked. Yet, these mechanisms are of  
107 importance because the crosstalk between gut epithelial cells and endothelium involves  
108 triggering of signaling pathways of immune and inflammation responses, which are key  
109 modulators of endothelial dysfunction [17,18].

110 In this work, we have evaluated the use of an *in vitro* co-culture model combining  
111 absorption effects with changes in endothelial function for the investigation of cellular  
112 responses after RSV treatment. Oxidative stress and the secretion of endothelial markers  
113 were evaluated under inflammatory and non-inflammatory conditions induced by TNF- $\alpha$ . In  
114 addition, shifts in RSV metabolism were investigated using LC-MS/MS<sup>E</sup> and correlated with  
115 the observed bioactive effects.

## 116 117 **2 Materials and Methods**

### 118 119 **2.1 Cell lines and cell culture**

120  
121 The experiments were performed using the continuous cell line Caco-2 (HTB-37<sup>TM</sup>,  
122 ATCC, Manassas, VA, USA), which differentiates into enterocyte-like cells upon  
123 confluency, and the permanent human endothelial cell line EAhy926 (CRL2922<sup>TM</sup>, ATCC).  
124 This endothelial cell line was chosen because of its continuous character, resulting in a fast  
125 and constant growth rate and more consistent response compared to primary cell lines such as

126 HUVEC. The Caco-2 cells (passage 15–27) and endothelial cells (passage 9–15) were grown  
127 separately as adherent cultures in 25 cm<sup>2</sup> tissue culture flasks (Sarstedt, Essen, Belgium) and  
128 cultivated in Dulbecco's modified Eagle's growth medium (DMEM), high glucose,  
129 supplemented with glutamax<sup>TM</sup>, sodium pyruvate, 10% (v/v) fetal bovine serum (Greiner bio-  
130 one, Wemmel, Belgium), penicillin (100 U/ml), and streptomycin (100mg/ml) (Gibco, Life  
131 Technologies, Ninove, Belgium). Cells were subcultured once a week with 0.25% (v/v)  
132 trypsin-EDTA and grown until 90% confluence. The culture medium was replaced every  
133 other day. Cells were incubated at 37 °C and 10% CO<sub>2</sub> in a water saturated atmosphere.

134

## 135 **2.2 Assays for mitochondrial activity**

136

137 Cellular mitochondrial activity after treatment with *trans*-resveratrol (RSV, 99%  
138 purity) (Sigma-Aldrich, St. Louis, MO, USA) was measured using the MTT assay (3-[4,5-  
139 dimethylthiazol-2-yl]-2,5 diphenyl tetrazolium bromide) (Sigma-Aldrich), as previously  
140 described [19]. Caco-2 and endothelial cells were seeded in 96-well plates at a concentration  
141 of 20,000 cells per well. Upon 100% confluency, cells were treated with serum-free exposure  
142 medium spiked with RSV at a concentration range of 1-100 μM and incubated at 37 °C, 10%  
143 CO<sub>2</sub>. The MTT test was performed after 3-days treatment for differentiated Caco-2 cells and  
144 2-days treatment for endothelial cells. Absorbance was measured at 570 nm using a Bio-Rad  
145 multiplate reader (Bio-Rad Laboratories, Hercules, CA, USA). Results are expressed as % of  
146 mitochondrial activity compared to untreated cells.

147

## 148 **2.3 Experimental setup: co-culture, sequential and standard culture**

149

150 Three types of experimental setups were used: (i) co-culture of Caco-2 cells with  
151 EA.hy926 cells, (ii) sequential culture of Caco-2 cells with EA.hy926 cells and (iii) standard  
152 culture which is a monoculture of EA.hy629 cells. (i) For the co-culture setup, Caco-2 cells  
153 were seeded on 12-well Transwell plates (0.4  $\mu\text{m}$  pore diameter, Elscolab, Kruibeke,  
154 Belgium) at a concentration of 250,000 cells per well. Fifteen days after confluency of the  
155 Caco-2 cells, EA.hy926 cells were seeded on the basolateral compartment of the Transwell  
156 plate, at a cell density of 300,000 cells per well. The EA.hy926 cells were grown in the co-  
157 culture system until they reached confluency on the third day. On the fourth day of co-  
158 culture, Caco-2 cells were treated apically with RSV in phenol-red free and serum-free  
159 exposure medium at concentrations of 5  $\mu\text{M}$  and 20  $\mu\text{M}$ , and RSV-free exposure medium  
160 was applied in the basolateral compartment. A concentration of 5  $\mu\text{M}$  was chosen because it  
161 is in the same range of peak plasma concentrations after moderate wine and juice  
162 consumption as reported previously [20-22], and consequently, 20  $\mu\text{M}$  is expected to be in  
163 the range of concentrations to which the gut epithelium is exposed to. Prior to RSV  
164 treatment, the basolateral compartment in the co-culture was incubated for 1 h with 10 ng/ml  
165  $\text{TNF-}\alpha$  in exposure medium in order to induce the high-grade inflammation associated with  
166 cardiovascular diseases. The co-culture was incubated at 37°C at 10%  $\text{CO}_2$  and samples of  
167 culture medium of apical and basal compartments were collected after 4 h, to study short  
168 term effects [18], and after 24 h – to observe longer term effects – and immediately stored at  
169 -80 °C prior to analysis.

170 (ii) Additionally, the same set of experiments was performed in a sequential setup to  
171 investigate the effects of RSV on cellular responses in an isolated system. For the sequential  
172 setup, Caco-2 cells were cultivated on Transwell inserts and allowed to differentiate for 15  
173 days after confluency, and EA.hy926 cells were seeded in a separate 24-well plate at a  
174 concentration of 100,000 cells per well. Prior to treatment at confluency, the endothelial cells

175 were treated with or without TNF- $\alpha$  as described before. EA.hy926 cells were incubated  
176 overnight either with the basolateral (transported) fraction collected at time points of 4 h and  
177 24 h after RSV treatment of Caco-2 cells or with RSV standard solutions in exposure  
178 medium (5  $\mu$ M and 20  $\mu$ M). (iii) In the standard setup, only endothelial cells were pretreated  
179 with TNF- $\alpha$  and incubated with the RSV standard solutions.

#### 181 **2.4 Lucifer Yellow permeability test and TEER measurement**

182  
183 For all transport experiments, the apparent permeability coefficient ( $P_{app}$ ) of Caco-2  
184 cell monolayers were monitored before and after the experiments using the fluorescent  
185 reagent Lucifer yellow (Sigma-Aldrich, Diegem, Belgium) as a indicative marker of passive  
186 paracellular diffusion [23]. In addition, the integrity of the Caco-2 cell monolayer was  
187 monitored before and after the experiments using transepithelial electrical resistance (TEER)  
188 measurements with an automated tissue resistance measurement system (REMS, World  
189 Precision Instruments, Hertfordshire, UK). Only intact Caco-2 monolayers with TEER values  
190 of 900-1100  $\Omega$  cm<sup>2</sup> were used for the co-culture experiments.

#### 192 **2.5 High resolution mass spectrometry analysis (UPLC-HDMS/MS<sup>E</sup>) analysis of** 193 **resveratrol metabolites**

194  
195 LC-MS/MS analysis was performed with a Waters Acquity UPLC system (Waters  
196 Corp., Milford, MA, USA) connected to a Synapt HDMS TOF mass spectrometer (Waters  
197 Corp.). LC separation was done on a Waters Acquity BEHC18 column (2.1 mm  $\times$  150 mm,  
198 1.7  $\mu$ m particle size) using gradient elution composed of (A) water (0.1% (v/v) formic acid)  
199 and (B) methanol (0.1% (v/v) formic acid) as earlier described [24]. The eluent was then



1  
2  
3  
4  
5  
6  
7  
8  
9  
10  
11  
12  
13  
14  
15  
16  
17  
18  
19  
20  
21  
22  
23  
24  
25  
26  
27  
28  
29  
30  
31  
32  
33  
34  
35  
36  
37  
38  
39  
40  
41  
42  
43  
44  
45  
46  
47  
48  
49  
50  
51  
52  
53  
54  
55  
56  
57  
58  
59  
60  
61  
62  
63  
64  
65

200 directed to the mass spectrometer equipped with electrospray ionization (ESI) source. Data  
201 were acquired in continuum negative ionization in V-mode. For MS/MS analysis, collision  
202 energies were set at 6 V for the low energy and 45 V for high energy. Mass range was set at  
203 100–1500 Da with a scan speed of 0.2 s per scan using the MassLynx software 4.1 (Waters  
204 Corp.). Metabolynx™, which was embedded within the MassLynx package was used to  
205 perform automated peak detection and identification of phase I and II metabolites.

206

## 207 **2.6 Determination of intracellular reactive oxygen species (ROS)**

208

209 The inhibition of intracellular ROS was monitored in endothelial cells through the  
210 reaction with the oxidant sensitive fluorogenic probe H<sub>2</sub>-DCFDA (2,7-  
211 dichlorodihydrofluorescein diacetate) (Sigma-Aldrich, St. Louis, MO, USA). The non-  
212 fluorogenic compound is converted by intracellular deacetylases to DCFH, which upon  
213 oxidation by ROS is converted to the highly fluorescent 2',7'-dichlorofluorescein (DCF) [25].  
214 After the transport experiments with RSV at 5 μM and 20 μM, endothelial cells were  
215 incubated with 20 μM H<sub>2</sub>-DCFDA in exposure medium for 30 min. The cells were then  
216 washed with phosphate buffered saline (PBS) and lysed with cold ultrapure water 10%  
217 ethanol for 30 min. The samples were then centrifuged at 10000 x g for 10 min, and  
218 fluorescence of supernatants was immediately measured on a Spectramax Fluorescent Plate  
219 Reader ( $\lambda_{ex/em}$ =485/535 nm) (Molecular Devices, CA, USA).

220

## 221 **2.7 Determination of nitric oxide (NO) production in endothelial cells**

222

223 The production of NO in endothelial cells was monitored using the Griess  
224 colorimetric assay (Sigma-Aldrich), as previously described [9]. Concentrations of nitrite

1  
2  
3  
4  
5  
6  
7  
8  
9  
10  
11  
12  
13  
14  
15  
16  
17  
18  
19  
20  
21  
22  
23  
24  
25  
26  
27  
28  
29  
30  
31  
32  
33  
34  
35  
36  
37  
38  
39  
40  
41  
42  
43  
44  
45  
46  
47  
48  
49  
50  
51  
52  
53  
54  
55  
56  
57  
58  
59  
60  
61  
62  
63  
64  
65

225 (NO<sub>2</sub>) were quantified through a six-point matrix-matched standard curve of sodium nitrite  
226 (NaNO<sub>2</sub>) (0-20 μmol/L). In the procedure, samples of culture medium were mixed with an  
227 equal volume of the Griess reagent. After 15 min at room temperature (18 °C), absorbance  
228 was read at 540 nm.

229

## 230 **2.8 Determination of inflammation markers by enzyme-linked immunosorbent**

### 231 **assays (ELISA)**

232

233 The cellular secretion of IL-8, VEGF and ICAM-1 in the co-culture was determined  
234 in cell culture media collected at time points 4 h and 24 h from the basolateral compartment  
235 and analysed using the human IL-8 TMB, human VEGF TMB and human ICAM-1 ABTS  
236 ELISA kits (Peprotech, London, UK), respectively, following the manufacturer's  
237 instructions.

238

## 239 **2.9 Statistical analysis**

240

241 Data were analyzed using one-way analysis of variance (ANOVA) followed by  
242 Student's *t*-test to assess statistical differences from control values and between  
243 inflammatory and non-inflammatory conditions (Statistica 7.0 203, StatSoft Inc., Tulsa,  
244 USA). Statistical significance was regarded at  $p < 0.05$  or  $p < 0.001$ . Results are expressed as  
245 mean ± standard error of mean (SEM). All experiments were carried out with three plates  
246 seeded at three different time points in the course of four months, comprising the biological  
247 replicates. For each biological replicate, results of three technical replicates were obtained.

248

## 249 **3 Results**

250

### 251 3.1 Identification of transported metabolites

252

253 The transport and metabolism of RSV by Caco-2 cells were tested in samples of  
254 basolateral media periodically collected between 0 h and 24 h. Upon 2 h exposure to 100  $\mu$ M  
255 RSV, the presence of RSV and a hydrophilic metabolite was detected in the chromatogram.  
256 Upon further incubation, RSV and other three metabolites were detected after 24h incubation  
257 (data not shown). Hence, for the MS/MS<sup>E</sup> analyses, the time point of 24 h was selected as  
258 optimized condition for identification of metabolites. Four monoconjugated metabolites were  
259 identified, comprising two sulfates and two glucuronides derivatives of RSV (Table 1). Fig. 1  
260 shows the MS spectra and extracted ion chromatogram of a cell culture medium sample  
261 collected after 24 h incubation and transport by Caco-2 cells treated with 20  $\mu$ M RSV.

262 In Fig. 1, MS data collected for RSV precursor and product ions shows the peaks of  
263 RSV and its main conjugated metabolites, confirmed based on the accurate mass of  $m/z$   
264 transition and retention time (rt): *trans*-resveratrol (rt = 23.53), *trans*-resveratrol-4'-*O*- $\beta$ -  
265 glucuronide (rt = 15.85), *trans*-resveratrol-4'-sulfate (rt = 17.23), *trans*-resveratrol-3-sulfate  
266 (rt = 20.19), *trans*-resveratrol-3-*O*- $\beta$ -glucuronide (rt = 20.58). Although less abundant, the  
267 presence of an ion peak of RSV reveals that not only RSV conjugates, but also the  
268 polyphenol in its intact form, is transported by Caco-2 cells. The hydrophilic metabolites  
269 produced well-separated and well-defined peaks, at the retention time range of 15.0-21.0  
270 min, with the highest intensity of sulfate metabolites. The MS spectra allowed a more  
271 accurate view of metabolites  $m/z$  transition, confirming the higher intensity of glucurono- and  
272 sulfo-conjugated derivatives in comparison with the parent compound. Also, the greater  
273 relative abundance of sulfated forms ( $m/z = 307.03$ ) compared to the parent and glucuronide

1  
2  
3  
4  
5  
6  
7  
8  
9  
10  
11  
12  
13  
14  
15  
16  
17  
18  
19  
20  
21  
22  
23  
24  
25  
26  
27  
28  
29  
30  
31  
32  
33  
34  
35  
36  
37  
38  
39  
40  
41  
42  
43  
44  
45  
46  
47  
48  
49  
50  
51  
52  
53  
54  
55  
56  
57  
58  
59  
60  
61  
62  
63  
64  
65

274 ions revealed that sulfates are the main conjugates formed during Caco-2 metabolism of  
275 RSV.

276

### 277 **3.2 Establishment of the co-culture characteristics and effect of RSV on cellular** 278 **mitochondrial activity**

279

280 To develop an *in vitro* model combining polyphenol absorption and effects on target  
281 tissue metabolism, differentiated Caco-2 cells were co-cultured with EA.hy926 cells and  
282 changes in permeability and cellular metabolism were monitored through mitochondrial  
283 activity in response to RSV in both TNF- $\alpha$  activated and non-activated cells. Regarding  
284 permeability,  $P_{app}$  values of apical-to-basolateral direction ranged from  $4.61 \pm 0.25 \times 10^{-5}$   
285 cm/s in the sequential system, composed of Caco-2 cells, to  $4.80 \pm 0.23 \times 10^{-5}$  cm/s in the co-  
286 culture system, composed of Caco-2 cells and EAhy926 cells in apical and basolateral  
287 compartments, respectively. The TEER values ranged from  $944.4 \pm 28.0 \Omega \text{ cm}^2$  in the  
288 sequential system to  $1034.8 \pm 43.9 \Omega \text{ cm}^2$  in the co-culture. The integrity and permeability  
289 variables were negatively correlated and no significant difference was found between both  
290 systems ( $p < 0.05$ ). We can therefore conclude that co-culture of Caco-2 and EA.hy926 cells,  
291 as well as the TNF- $\alpha$  and RSV treatments, did not negatively affect the Caco-2 intestinal  
292 barrier integrity.

293 In contrast, changes in mitochondrial activity in response to RSV were largely  
294 influenced by cultivation method, with distinct responses observed in the co-culture,  
295 compared to sequential and standard culture methods (Fig. 2). A first observation is that only  
296 in the co-culture system after 24 h, the mitochondrial activity of TNF- $\alpha$  treated endothelial  
297 cells was significantly decreased by about 35% compared to the untreated cells, which was  
298 independent of RSV concentration. This effect was not visible in the sequential setup, where

1  
2  
3  
4  
5  
6  
7  
8  
9  
10  
11  
12  
13  
14  
15  
16  
17  
18  
19  
20  
21  
22  
23  
24  
25  
26  
27  
28  
29  
30  
31  
32  
33  
34  
35  
36  
37  
38  
39  
40  
41  
42  
43  
44  
45  
46  
47  
48  
49  
50  
51  
52  
53  
54  
55  
56  
57  
58  
59  
60  
61  
62  
63  
64  
65

299 only the endothelial cells have received the TNF- $\alpha$  treatment. Therefore, we may conclude  
300 that, upon TNF- $\alpha$  treatment, the Caco-2 cells secrete RSV-independent cytokines that  
301 damage the endothelium after 24 h.

302 A second observation is that under standard monoculture conditions, RSV increased  
303 mitochondrial activity in a dose-dependent way, which was most probably not the result of  
304 cell proliferation, as the total protein content of the wells, as measured with a sulforhodamin  
305 B (SRB) test, was not increased in parallel. The mitochondrial increase was not visible in the  
306 co-culture system, and also in the sequential setup no clear trend could be seen. This may be  
307 a first indication that native RSV, but not the transported conjugated metabolites, increases  
308 mitochondrial activity *in vitro*. Third, in general, trends of RSV treatment at different  
309 concentrations in the co-culture and sequential system after 4 and 24 hours are similar. More  
310 specifically, 5  $\mu$ M RSV gave a slightly increased reactivity, whereas a slight decrease was  
311 observed at 20  $\mu$ M. This observation illustrates that RSV induced cell signaling pathways  
312 may be concentration dependent. This reactivity was probably not related to apoptotic  
313 pathway induction, as in preliminary experiments, we verified that incubation of Caco-2 and  
314 EA.hy926 cells with similar RSV concentrations for three days did not result in cell toxicity.

315

### 316 **3.3 NO production**

317

318 The effect of RSV and its metabolites on cellular NO production is presented in Fig.  
319 3. First, a 1-hour TNF- $\alpha$  pretreatment of cells resulted in significantly higher NO levels in the  
320 co-culture and sequential setup, especially after 24 h. Interestingly, this effect was not visible  
321 for the standard conditions. A second observation is that under standard as well as co-culture  
322 conditions, a concentration of 20  $\mu$ M significantly increased NO production after 4 and 24 h  
323 of treatment with RSV, and in both TNF- $\alpha$  treated and untreated conditions. This is

1  
2  
3  
4  
5  
6  
7  
8  
9  
10  
11  
12  
13  
14  
15  
16  
17  
18  
19  
20  
21  
22  
23  
24  
25  
26  
27  
28  
29  
30  
31  
32  
33  
34  
35  
36  
37  
38  
39  
40  
41  
42  
43  
44  
45  
46  
47  
48  
49  
50  
51  
52  
53  
54  
55  
56  
57  
58  
59  
60  
61  
62  
63  
64  
65

324 consistent with literature for monoculture systems [9, 13]. However, at lower concentrations  
325 of RSV (5  $\mu$ M), NO production was significantly reduced at 4 h and slightly reduced at 24 h,  
326 in the non-inflammatory condition.

327 Third, it could be observed that especially under TNF- $\alpha$  induced conditions, addition  
328 of RSV resulted in extra NO production in a dose-dependent way, but only in the co-culture  
329 and sequential setup. This may indicate that either the transported fraction containing RSV  
330 and its Caco-2 derived metabolites, rather than the polyphenol alone, improves NO  
331 production by the endothelial cells, or that NO is also produced by Caco-2 cells in response  
332 to RSV, or both.

333

#### 334 **3.4 RSV and metabolites inhibit oxidative stress in co-culture and sequential models**

335

336 First, a one-hour treatment of the cells with TNF- $\alpha$  resulted in a strong increase in  
337 intracellular ROS in all setups, reaching 4-fold concentrations in the co-culture setup after 4  
338 h (Fig. 4), which corresponds with literature data [18]. Secondly, when cells were pretreated  
339 with TNF- $\alpha$ , the increase in ROS was strongly dependent on the experimental setup. The  
340 fastest response was visible for the endothelial cells in the co-culture setup, as values were  
341 higher at 4 h compared to 24 h of incubation. The opposite was observed for the sequential  
342 setup, whereas the effect on standard monoculture setup was rather limited. Together with  
343 the MTT results, we conclude that the fast and strong oxidative response in the TNF- $\alpha$   
344 stimulated co-culture setup has most probably led to permanent endothelial damage after 24  
345 h caused by Caco-2 secreted factors.

346 Thirdly, the effect of RSV on ROS was dependent on both TNF- $\alpha$  treatment and  
347 experimental setup. Under non-inflammatory conditions, the effect of RSV was only  
348 significant in the co-culture model. At 5  $\mu$ M RSV, intracellular levels of ROS were

1  
2  
3  
4  
5  
6  
7  
8  
9  
10  
11  
12  
13  
14  
15  
16  
17  
18  
19  
20  
21  
22  
23  
24  
25  
26  
27  
28  
29  
30  
31  
32  
33  
34  
35  
36  
37  
38  
39  
40  
41  
42  
43  
44  
45  
46  
47  
48  
49  
50  
51  
52  
53  
54  
55  
56  
57  
58  
59  
60  
61  
62  
63  
64  
65

349 significantly reduced after 4 h incubation, showing a late increase after 24 h incubation. For  
350 20  $\mu$ M RSV, the ROS levels in endothelial cells were consistently lower up to 24 h  
351 incubation in the co-culture model. Under inflammatory conditions, RSV treatment gave a  
352 dose-dependent decrease of ROS in the co-culture setup after 4 h, whereas the opposite was  
353 true for the sequential setup. After 24 h, this dose-response effect was less visible. These  
354 results indicate that addition of RSV in the co-culture setup may effectively reduce the  
355 oxidative stress induced in the endothelial cells by TNF- $\alpha$  and cytokines produced by the  
356 Caco-2 cells.

357

### 358 **3.5 RSV affects inflammation markers in the co-culture**

359

360 The secretion of proinflammatory markers was tested in both TNF- $\alpha$ -treated and  
361 untreated cells in order to determine RSV effects on endothelium responses under  
362 inflammatory and non-inflammatory conditions, respectively. Considering the results of  
363 oxidative parameters, we have chosen the co-culture model to study the influence of RSV on  
364 secretion of markers VEGF, ICAM-1 and IL-8. Changes in cytokine expression may  
365 therefore be caused by both cell types.

366 In TNF- $\alpha$ -activated cells, the secretion of markers was significantly higher in  
367 comparison with basal values of the non-inflammatory condition (Fig. 5), and increased  
368 concentrations of 1.5-fold up to 7-fold were verified for the adhesion ICAM-1 (107.10  
369 pg/ml) and IL-8 (75.23 pg/ml) proteins, respectively. Concentrations of VEGF in the medium  
370 ranged from 12.06 to 236.44 pg/ml for untreated cells (blank) of the non-inflammatory and  
371 inflammatory conditions, respectively.

372 Under healthy conditions, the overall concentration of IL-8 (10.95 pg/ml)  
373 significantly decreased in a dose-dependent way in co-cultured cells treated with RSV at 5

1  
2  
3  
4  
5  
6  
7  
8  
9  
10  
11  
12  
13  
14  
15  
16  
17  
18  
19  
20  
21  
22  
23  
24  
25  
26  
27  
28  
29  
30  
31  
32  
33  
34  
35  
36  
37  
38  
39  
40  
41  
42  
43  
44  
45  
46  
47  
48  
49  
50  
51  
52  
53  
54  
55  
56  
57  
58  
59  
60  
61  
62  
63  
64  
65

374  $\mu\text{M}$  (8.09 pg/ml) and 20  $\mu\text{M}$  (9.40 pg/ml). Upon TNF- $\alpha$  activation, the secretion of IL-8  
375 consistently reduced from 4 h to 24 h in cells exposed to RSV compared to the untreated  
376 cells. Remarkably, unlike VEGF and ICAM, the values of IL-8 under inflammatory  
377 conditions were higher after 4 hours compared to 24 h of treatment. These results indicate  
378 that, in contrast with the other tested chemokines, there was no constant accumulation of IL-8  
379 in the medium over time, and that IL-8 may be bound to receptors, such as G-protein  
380 coupled receptors, which are present in both cell types [26,27]. Secondly, under normal  
381 conditions, RSV decreased VEGF secretion in a dose dependent way at 24h of treatment.  
382 Under TNF- $\alpha$  induced conditions, however, a dose-dependent increase of VEGF was  
383 observed after 4 h of treatment. After 24 hours, the trend was less visible. ICAM-1  
384 expression significantly increased upon TNF- $\alpha$  stimulation. Interestingly, ICAM-1 was about  
385 6-fold higher after 24 h of incubation, which corresponds with the time-point in which the  
386 mitochondrial activity of the endothelial cells was significantly reduced. Though some  
387 conditions showed an effect of RSV on ICAM-1 expression, no clear dose-dependent  
388 correlation could be observed.

389

#### 390 **4 Discussion**

391

392 This study assessed the impact of *trans*-resveratrol and metabolites on key markers of  
393 mitochondrial activity, oxidative stress and inflammation associated with endothelial  
394 dysfunction in an *in vitro* cell culture setup that allowed intestinal metabolism and crosstalk  
395 between intestinal and endothelial cells. Though a similar co-culture model was developed  
396 recently [18], we have performed a more in-depth study on the value of our co-culture model  
397 compared to the conventionally used sequential and monoculture models. Besides this, major  
398 differences between the previously published model and the one discussed in this paper are



1  
2  
3  
4  
5  
6  
7  
8  
9  
10  
11  
12  
13  
14  
15  
16  
17  
18  
19  
20  
21  
22  
23  
24  
25  
26  
27  
28  
29  
30  
31  
32  
33  
34  
35  
36  
37  
38  
39  
40  
41  
42  
43  
44  
45  
46  
47  
48  
49  
50  
51  
52  
53  
54  
55  
56  
57  
58  
59  
60  
61  
62  
63  
64  
65

399 (i) the cell lines used for the co-culture, (ii) some of the biological endpoints, (iii) the use of  
400 resveratrol instead of a mixed grape anthocyanin extract and (iv) a detailed analysis of  
401 resveratrol metabolites that were actually reaching the endothelial cell compartment. When  
402 comparing our co-culture setup with the sequential and monoculture, evidence for crosstalk  
403 can be drawn from our results. Changes in ROS and NO levels in the co-culture  
404 demonstrated a clear effect of the communication between cell lines. Upon inflammation, the  
405 consistent decays on mitochondrial activity and intracellular ROS indicated damage of the  
406 endothelial cells due to oxidative mechanisms and the combined metabolism in the co-  
407 culture. This damage could be delayed by RSV, but not restored.

408         When comparing our co-culture model with the one previously reported [18], we  
409 have found some similarities. In fact, TNF- $\alpha$  exerted a strong inducible effect on the  
410 secretion of the adhesion molecule and proinflammatory chemokines in the co-culture. Also,  
411 this effect was more pronounced after the long-term incubation of 24 h. We evaluated RSV  
412 effects on secretion of VEGF, IL-8 and ICAM-1 in the co-culture model, in TNF- $\alpha$ -activated  
413 and non-activated cells. Diverse stimuli affecting NO regulation and ROS formation may  
414 lead to expression of these proinflammatory molecules in endothelium [28]. As expected,  
415 secretion of the endothelial growth factor, IL-8 cytokine and the adhesion molecule were  
416 largely increased by induction of inflammation with TNF- $\alpha$ . In fact, TNF- $\alpha$  modulates the  
417 expression of up to 4,000 genes in endothelial cells, most related to cell adhesion,  
418 inflammation and chemotaxis proteins [29]. We observed that upon exposure to TNF- $\alpha$ ,  
419 levels of VEGF, NO and ROS were significantly increased in the co-culture. This effect may  
420 be explained by activation of mitochondrial Romo1 receptor, boosting ROS formation; and  
421 by upregulation of VEGF synthesis in endothelial cells, causing stimulation of the tyrosine  
422 kinase receptor VEGFR/Flt (KDR) involved in eNOS phosphorylation and NO activation  
423 [30,31]. In addition, VEGF, as well as IL-8 and ICAM-1 expression may be the result of

1  
2  
3  
4  
5  
6  
7  
8  
9  
10  
11  
12  
13  
14  
15  
16  
17  
18  
19  
20  
21  
22  
23  
24  
25  
26  
27  
28  
29  
30  
31  
32  
33  
34  
35  
36  
37  
38  
39  
40  
41  
42  
43  
44  
45  
46  
47  
48  
49  
50  
51  
52  
53  
54  
55  
56  
57  
58  
59  
60  
61  
62  
63  
64  
65

424 TNF- $\alpha$ -induced activation of NF- $\kappa$ B [32,33]. Despite the significant effect of RSV and its  
425 metabolites on reducing secretion of proinflammatory molecules in the co-culture, decreases  
426 on ICAM-1, VEGF and IL-8 concentrations in relation to each control were more  
427 pronounced in TNF- $\alpha$ -activated cells. Thus, suggesting that RSV and its metabolites operate  
428 through an inhibitory regulation of the inflammatory cascade in endothelial cells, which can  
429 maintain a more sustained effect under pre-existing inflammation.

430         Compared to the HUVEC cells in a co-culture [18], the EA.hy926 cell line used in  
431 this study has the advantage that it is an immortalized cell line with endothelial  
432 characteristics, and therefore are easy to cultivate without loss of growth and function over  
433 time. However, this cell line is the fusion product of primary umbilical vein cells with the  
434 A549 lung carcinoma cell line, and therefore, we can not rule out that some of the responses  
435 are driven by its cancerous origin. Yet, the co-culture system has the potential to mimic the *in*  
436 *vivo* conditions because of the following reasons; (i) the close proximity in a non-contact  
437 setup between the apical and basal cells mimicking the gut epithelial cells and target tissues;  
438 (ii) the Caco-2 cells in the apical compartment simulates the intestinal barrier as the first line  
439 of contact to the intestinal lumen in order to absorb dietary compounds; (iii) the direct  
440 communication between cell lines is affected by soluble mediators secreted by both cell types  
441 [17]. Therefore, we conclude that this model is able to study the impact of absorbed bioactive  
442 compounds on the endothelium.

443         Concerning the biological endpoints, we have studied endpoints of oxidative stress  
444 and inflammation. *In vivo*, this situation happens when there is an imbalance of oxidation  
445 mediators and antioxidant defenses [3,28]. Resveratrol has the potential to beneficially  
446 impact this situation [8,30]. In our results, RSV strongly influenced NO production in cells  
447 under healthy and unhealthy condition. Indeed, RSV has been reported to positively induce  
448 endothelial nitric oxide synthase (eNOS) activity and NO release in endothelial cells [34].

1  
2  
3  
4  
5  
6  
7  
8  
9  
10  
11  
12  
13  
14  
15  
16  
17  
18  
19  
20  
21  
22  
23  
24  
25  
26  
27  
28  
29  
30  
31  
32  
33  
34  
35  
36  
37  
38  
39  
40  
41  
42  
43  
44  
45  
46  
47  
48  
49  
50  
51  
52  
53  
54  
55  
56  
57  
58  
59  
60  
61  
62  
63  
64  
65

449 Resveratrol promotes NO activation through stimulation of phosphorylation of protein kinase  
450 B and vasodilator-activated protein (VASP) [11]. However, neither resveratrol sulfates nor  
451 glucuronides were able to induce NO release in endothelial cells [35]. Markedly, our results  
452 showed that ROS levels were only significantly reduced in the co-culture, after metabolism  
453 of RSV by Caco-2 cells.

454         During absorption, RSV undergoes excessive metabolism by gut epithelial cells,  
455 whereas only very low amounts of unconjugated resveratrol are circulating in the blood  
456 stream. The sulfated and glucuronated conjugates are present in larger amounts [8,36]. These  
457 conjugates were also found in our setup using LC-MS/MS, thereby confirming the value of  
458 using an intestinal cell culture in this *in vitro* study design. The MS analysis revealed four  
459 RSV conjugates produced through sulfation and glucuronidation processes of phase II  
460 metabolism by Caco-2, comprising two sulfate derivatives and two glucuronide metabolites.  
461 These are, in fact, the main metabolic conjugates of *trans*-resveratrol [36]. Moreover,  
462 endothelial cells treated with either the unconjugated polyphenol in the monoculture standard  
463 setup clearly behaved differently from the endothelial cells treated with basal medium after  
464 Caco-2 transport of RSV. This may be due to the low bioactivity of conjugated RSV  
465 metabolites as well as to other factors secreted by the Caco-2 cells during cellular  
466 metabolism. Indeed, previous literature suggest the low bioavailability of the parent  
467 polyphenol and lack of bioactivity of RSV metabolites [6,16]. Finally, no shifts in RSV  
468 metabolism as a result of TNF- $\alpha$  treatment could be observed, which indicates that the  
469 contact time of the endothelial cells with TNF- $\alpha$  was insufficient to induce crosstalk  
470 mechanisms that could regulate polyphenol uptake and metabolism by the cells.

471

## 472 **5         Conclusions**

473

1  
2  
3  
4  
5  
6  
7  
8  
9  
10  
11  
12  
13  
14  
15  
16  
17  
18  
19  
20  
21  
22  
23  
24  
25  
26  
27  
28  
29  
30  
31  
32  
33  
34  
35  
36  
37  
38  
39  
40  
41  
42  
43  
44  
45  
46  
47  
48  
49  
50  
51  
52  
53  
54  
55  
56  
57  
58  
59  
60  
61  
62  
63  
64  
65

474 This study demonstrated that RSV and its metabolites exert a protective effect in  
475 endothelial cells against oxidative stress and inflammation, which are intimately associated to  
476 cardiovascular diseases. This effect was verified in endothelial cells cultivated in both co-  
477 culture with intestinal cells (Caco-2) and sequential systems (post-transport), under  
478 inflammatory and non-inflammatory conditions. Notwithstanding, we demonstrated for the  
479 first time the bioactivity of RSV and of its sulfate and glucuronide metabolites in a co-culture  
480 towards TNF- $\alpha$ -induced endothelial dysfunction. It was evidenced that the metabolism of  
481 endothelial cells as a biological target is not only influenced by polyphenol intervention, but  
482 also influenced by the communication between distinct cell lines.

483

#### 484 **Acknowledgements**

485

486 *The authors acknowledge the financial support of the BOF Special Research Fund*  
487 *(project 01B04212), Hercules Project (AUGE028 and AUGE014) and the Brazilian National*  
488 *Council for Scientific and Technological Development (CNPq) (grant 248460/2013-7 to*  
489 *I.M.T.).*

490

#### 491 **Author's contribution**

492

493 I.M.T., J.V.C., M.T.B.L. and C.G. contributed to the design of the project, cell  
494 experiments and development of the co-culture and the manuscript; G.B.G., S.K., G.S., K.R.  
495 and E.C. contributed to the methodology of metabolites identification, cell experiments and  
496 UPLC-MS/MS analysis of metabolites. All authors contributed to writing and revision of the  
497 manuscript.

498

1  
2  
3  
4  
5  
6  
7  
8  
9  
10  
11  
12  
13  
14  
15  
16  
17  
18  
19  
20  
21  
22  
23  
24  
25  
26  
27  
28  
29  
30  
31  
32  
33  
34  
35  
36  
37  
38  
39  
40  
41  
42  
43  
44  
45  
46  
47  
48  
49  
50  
51  
52  
53  
54  
55  
56  
57  
58  
59  
60  
61  
62  
63  
64  
65

499 **Conflict of interest**

500

501 *None declared.*

502

503 **References**

504

505 [1] Das M, Das DK. Resveratrol and cardiovascular health. *Mol Aspects Med* 2010;31:503–  
506 12.

507

508 [2] Libby P. Inflammation in atherosclerosis. *Nature* 2002;420:19–26.

509

510 [3] Hajjar DP, Gotto AM. Biological relevance of inflammation and oxidative stress in the  
511 pathogenesis of arterial diseases. *Am J Pathol* 2013;182:1474–81.

512

513 [4] Tabruyn SP, Mémet S, Avé P, Verhaeghe C, Mayo KH, Struman I, Martial JA, Griffioen  
514 AW. NF- $\kappa$ B activation in endothelial cells is critical for the activity of angiostatic agents.  
515 *Mol Cancer Ther* 2009;8:2645–54.

516

517 [5] Ruiz-Núñez B, Pruijboom L, Dijck-Brouwer DAJ, Muskiet FAJ. Lifestyle and  
518 nutritional imbalances associated with Western diseases: causes and consequences of chronic  
519 systemic low-grade inflammation in an evolutionary context. *J Nutr Biochem* 2013;24:1183–  
520 1201.

521

522 [6] Manach C, Scalbert A, Morand C, Rémésy C, Jiménez L. Polyphenols: food sources and  
523 bioavailability. *Am J Clin Nutr* 2004;79:727–47.

524

1  
2 525 [7] Gresele P, Cerletti C, Guglielmini G, Pignatelli P, Gaetano G, Violi F. Effects of  
3  
4 526 resveratrol and other wine polyphenols on vascular function: an update. *J Nutr Biochem*  
5  
6  
7 527 2011;22:201–11.

8  
9 528

10  
11 529 [8] Saiko P, Szakmary A, Jaeger W, Szekeres T. Resveratrol and its analogs: Defense against  
12  
13 530 cancer, coronary disease and neurodegenerative maladies or just a fad? *Mutat Res*  
14  
15  
16 531 2008;658:68–94.

17  
18  
19 532

20  
21 533 [9] Simão F, Pagnussat AS, Seo JH, Navaratna D, Leung W, Lok J, Guo S, Waeber C,  
22  
23 534 Salbego CG, Lo EH. Pro-angiogenic effects of resveratrol in brain endothelial cells: nitric  
24  
25 535 oxide-mediated regulation of vascular endothelial growth factor and metalloproteinases. *J*  
26  
27  
28 536 *Cereb Blood Flow Metab* 2012;32:884–95.

29  
30  
31 537

32  
33 538 [10] Zhang YQ, Liu YJ, Mao YF, Dong WW, Zhu XY, Jiang L. Resveratrol ameliorates  
34  
35 539 lipopolysaccharide-induced epithelial mesenchymal transition and pulmonary fibrosis  
36  
37  
38 540 through suppression of oxidative stress and transforming growth factor- $\beta$ 1 signaling. *Clin*  
39  
40  
41 541 *Nutr* 2015;34:752–60.

42  
43  
44 542

45  
46 543 [11] Gresele P, Pignatelli P, Guglielmini G, Carnevale R, Mezzasoma AM, Ghiselli A, Momi  
47  
48 544 S, Violi F. Resveratrol, at concentrations attainable with moderate wine consumption,  
49  
50 545 stimulates human platelet nitric oxide production. *J Nutr* 2008;138:1602–08.

51  
52  
53 546  
54  
55  
56  
57  
58  
59  
60  
61  
62  
63  
64  
65

- 1  
2  
3  
4  
5  
6  
7  
8  
9  
10  
11  
12  
13  
14  
15  
16  
17  
18  
19  
20  
21  
22  
23  
24  
25  
26  
27  
28  
29  
30  
31  
32  
33  
34  
35  
36  
37  
38  
39  
40  
41  
42  
43  
44  
45  
46  
47  
48  
49  
50  
51  
52  
53  
54  
55  
56  
57  
58  
59  
60  
61  
62  
63  
64  
65
- 547 [12] Nagai N, Kubota S, Tsubota K, Ozawa. Resveratrol prevents the development of  
548 choroidal neovascularization by modulating AMP-activated protein kinase in macrophages  
549 and other cell types. *J Nutr Biochem* 2014;25:1218–25.  
550
- 551 [13] Csiszar A, Smith K, Labinskyy N, Orosz Z, Rivera A, Ungvari Z. Resveratrol attenuates  
552 TNF- $\alpha$ -induced activation of coronary arterial endothelial cells: role of NF- $\kappa$ B inhibition.  
553 *Am. J Physiol Heart Circ Physiol* 2006;291:1694–99.  
554
- 555 [14] Thiel G, Rossler, OG. Resveratrol stimulates AP-1-regulated gene transcription. *Mol*  
556 *Nutr Food Res* 2014;58:1402–13.  
557
- 558 [15] Storniolo CE, Moreno JJ. Resveratrol metabolites have an antiproliferative effect on  
559 intestinal epithelial cancer cells. *Food Chem* 2012;134:1385–91.  
560
- 561 [16] Polycarpou E, Meira LB, Carrington S, Tyrrell E, Modjtahedi H, Carew MA.  
562 Resveratrol 3-O-D-glucuronide and resveratrol 4-O-D-glucuronide inhibit colon cancer cell  
563 growth: Evidence for a role of A3 adenosine receptors, cyclin D1 depletion, and G1 cell  
564 cycle arrest. *Mol Nutr Food Res* 2013;57:1708–17.  
565
- 566 [17] Maaser C, Schoeppner S, Kucharzik T, Kraft M, Schoenherr E, Domschke W,  
567 Luegering N. Colonic epithelial cells induce endothelial cell expression of ICAM-1 and  
568 VCAM-1 by a NF-kappaB-dependent mechanism. *Clin Exp Immunol* 2001;124:208–13.  
569

- 1  
2  
3  
4  
5  
6  
7  
8  
9  
10  
11  
12  
13  
14  
15  
16  
17  
18  
19  
20  
21  
22  
23  
24  
25  
26  
27  
28  
29  
30  
31  
32  
33  
34  
35  
36  
37  
38  
39  
40  
41  
42  
43  
44  
45  
46  
47  
48  
49  
50  
51  
52  
53  
54  
55  
56  
57  
58  
59  
60  
61  
62  
63  
64  
65
- 570 [18] Kuntz S, Asseburg H, Dold S, Römpf A, Fröhling B, Kunz C, Rudloff S. Inhibition of  
571 low-grade inflammation by anthocyanins from grape extract in an in vitro epithelial-  
572 endothelial co-culture model. *Food Funct* 2015;4:1136–49.  
573
- 574 [19] Notarnicola M, Pisanti S, Tutino V, Bocale D, Rotelli MT, Gentile A, Memeo V,  
575 Bifulco M, Perri E, Caruso MG. Effects of olive oil polyphenols on fatty acid synthase gene  
576 expression and activity in human colorectal cancer cells. *Genes Nutr* 2011;6:63–9.  
577
- 578 [20] Goldberg DM, Yan J, Soleas GJ. Absorption of three wine-related polyphenols in three  
579 different matrices by healthy subjects. *Clin Biochem* 2003;36:79–87.  
580
- 581 [21] Walle T, Hsieh F, Delegge MH, Oatis JE, Walle UK. High absorption but very low  
582 bioavailability of oral resveratrol in humans. *Drug Metab Dispos* 2004;32:1377–82.  
583
- 584 [22] Boocock DJ, Faust GE, Patel KR, et al. Phase I dose escalation pharmacokinetic study  
585 in healthy volunteers of resveratrol, a potential cancer chemopreventive agent. *Cancer*  
586 *Epidemiol Biomarkers Prev* 2007;16:1246–52.  
587
- 588 [23] Calatayud M, Gimeno J, Vélez D, Devesa V, Montoro R. Characterization of the  
589 intestinal absorption of arsenate, monomethylarsonic acid, and dimethylarsinic acid using the  
590 caco-2 cell line. *Chem Res Toxicol* 2010;23:547–56.  
591
- 592 [24] Gonzales GB, Raes K, Coelus S, Struijs K, Smagghe G, Van Camp J. Ultra (high)-  
593 pressure liquid chromatography–electrospray ionization–time-of-flight–ion mobility–high



1  
2  
3  
4  
5  
6  
7  
8  
9  
10  
11  
12  
13  
14  
15  
16  
17  
18  
19  
20  
21  
22  
23  
24  
25  
26  
27  
28  
29  
30  
31  
32  
33  
34  
35  
36  
37  
38  
39  
40  
41  
42  
43  
44  
45  
46  
47  
48  
49  
50  
51  
52  
53  
54  
55  
56  
57  
58  
59  
60  
61  
62  
63  
64  
65

594 definition mass spectrometry for the rapid identification and structural characterization of  
595 flavonoid glycosides from cauliflower waste. *J Chromatogr A* 2014;1323:39-48.  
596  
597 [25] Chiesi C, Fernandez-Blanco C, Cossignani L, Font G, Ruiz MJ. Alternariol-induced  
598 cytotoxicity in Caco-2 cells. Protective effect of the phenolic fraction from virgin olive oil.  
599 *Toxicon* 2015;93:103–11.  
600  
601 [26] Li A, Varney ML, Singh RK. Expression of interleukin 8 and its receptors in human  
602 colon carcinoma cells with different metastatic potentials1. *Clin Cancer Res*;7:3298–3304.  
603  
604 [27] Lai Y, Shen Y, Liu XH, Zhang Y, Zeng Y, Liu YF. Interleukin-8 induces the endothelial  
605 cell migration through the activation of phosphoinositide 3-kinase-Rac1/RhoA pathway. *Int J*  
606 *Biol Sci* 2011;7:782–791.  
607  
608 [28] Harrison DJ, Gongora MC. Oxidative stress and hypertension. *Med Clin N Am*  
609 2009;93:621–35.  
610  
611 [29] Claude S. Boby C, Rodriguez-Mateos A, Spencer JPE, Gérard N, Morand C,  
612 Milenkovic D. Flavanol metabolites reduce monocyte adhesion to endothelial cells through  
613 modulation of expression of genes via p38-MAPK and p65-Nf-kB pathways. *Mol Nutr Food*  
614 *Res* 2014;58:1016–27.  
615  
616 [30] Das S, Alagappan VKT, Bagchi D, Sharma HS, Maulik N, Das DK. Coordinated  
617 induction of iNOS–VEGF–KDR–eNOS after resveratrol consumption: A potential  
618 mechanism for resveratrol preconditioning of the heart. *Vascul Pharmacol* 2005;42:281–89.

619

1  
2 620 [31] Kim JJ, Lee SB, Park JK, Yoo YD. TNF- $\alpha$ -induced ROS production triggering  
3  
4 621 apoptosis is directly linked to Romo1 and Bcl-XL. Cell Death Differ 2010;17:1420–34.  
5  
6

7 622

8  
9 623 [32] Palomer X, Capdevila-Busquets E, Álvarez-Guardia D, Barroso E, Pallàs M, Camins A,  
10  
11 Davidson MM, Planavila A, Villarroya F, Vázquez-Carrera M. Resveratrol induces nuclear  
12 624 factor- $\kappa$ B activity in human cardiac cells. Int J Cardiol 2013;167:2507–16.  
13  
14 625  
15  
16

17 626

18  
19 627 [33] Zhang J, Peng B. In vitro angiogenesis and expression of nuclear factor  $\kappa\beta$  and VEGF in  
20  
21 628 high and low metastasis cell lines of salivary gland Adenoid Cystic Carcinoma. BMC Cancer  
22  
23 629 2007;7:95.  
24  
25

26 630

27  
28 631 [34] Penumathsa SV, Koneru S, Samuel SM, Maulik G, Bagchi D, Yet SF, Menon VP,  
29  
30 632 Maulik N. Strategic targets to induce neovascularization by resveratrol in  
31  
32 633 hypercholesterolemic rat myocardium: Role of caveolin-1, endothelial nitric oxide synthase,  
33  
34 634 hemeoxygenase-1, and vascular endothelial growth factor. Free Radical Biol Med  
35  
36 635 2008;45:1027–34.  
37  
38  
39  
40

41 636

42  
43 637 [35] Ladurner A, Schachner D, Schueller K, Pignitter M, Heiss EH, Somoza V, Dirsch VM.  
44  
45 638 Impact of trans-resveratrol-sulfates and -glucuronides on endothelial nitric oxide synthase  
46  
47 639 activity, nitric oxide release and intracellular reactive oxygen species. Molecules  
48  
49 640 2014;19:16724–36.  
50  
51  
52

53 641

54  
55 642 [36] Menet MC, Cottart CH, Taghi M, Nivet-Antoine V, Dargère D, Vibert F, Laprévotéa O,  
56  
57 643 Beaudeuxc J-L. Ultra high performance liquid chromatography-quadrupole-time of flight  
58  
59  
60  
61  
62  
63  
64  
65

644 analysis for the identification and the determination of resveratrol and its metabolites in  
645 mouse plasma. Anal Chim Acta 2013;761:128–36.

646

647

648 **Figure captions**

649

650 **Figure 1.** Representative MS/MS<sup>E</sup> chromatograms of the transported fraction after 24 h  
651 incubation of Caco-2 cells treated with RSV. Total ion chromatogram (A) of RSV and its  
652 metabolites: 1 = *trans*-resveratrol-4'-*O*- $\beta$ -glucuronide, 2 = *trans*-resveratrol-4'-sulfate, 3 =  
653 *trans*-resveratrol-3-sulfate, 4 = *trans*-resveratrol-3-*O*- $\beta$ -glucuronide, 5 = *trans*-resveratrol.

654 Extracted ion chromatogram of resveratrol (*m/z* 227.07) and its sulfate (*m/z* 307.03) (B) and  
655 glucuronide (*m/z* 403.11) (C) metabolites.

656

657 **Figure 2.** Mitochondrial activity of endothelial cells at 4 h (A) and 24 h (B) in response to  
658 RSV treatment in co-culture (black bars), sequential (dark grey bars) and standard (light grey  
659 bars) systems, under TNF- $\alpha$ -induced inflammatory and non-inflammatory conditions,  
660 expressed as percentage towards untreated cells without TNF- $\alpha$  addition. Results are  
661 expressed as percentage of the control condition that did not receive a RSV or TNF-  
662  $\alpha$  treatment. Data represent the mean  $\pm$  SEM, three measurements in triplicates, in three  
663 independent experiments. \* and \*\* indicate significant differences ( $p < 0.05$  and  $p < 0.001$ ,  
664 respectively) compared to the respective control sample without RSV treatment; and # and ##  
665 indicate significant differences ( $p < 0.05$  and  $p < 0.001$ , respectively) compared to the  
666 respective control sample without TNF- $\alpha$  treatment.

667

1  
2  
3  
4  
5  
6  
7  
8  
9  
10  
11  
12  
13  
14  
15  
16  
17  
18  
19  
20  
21  
22  
23  
24  
25  
26  
27  
28  
29  
30  
31  
32  
33  
34  
35  
36  
37  
38  
39  
40  
41  
42  
43  
44  
45  
46  
47  
48  
49  
50  
51  
52  
53  
54  
55  
56  
57  
58  
59  
60  
61  
62  
63  
64  
65

668 **Figure 3.** Effect of RSV and metabolites on NO production at 4h (A) and 24h (B) under  
669 TNF- $\alpha$ -induced inflammation and non-inflammatory condition, expressed as percentage  
670 towards untreated cells without TNF- $\alpha$  addition. Data expressed as mean  $\pm$  SEM of  
671 triplicates, in three independent experiments. \* and \*\* indicate significant differences  
672 ( $p<0.05$  and  $p<0.001$ , respectively) compared to the respective control sample without RSV  
673 treatment; and # and ## indicate significant differences ( $p<0.05$  and  $p<0.001$ , respectively)  
674 compared to the respective control sample without TNF- $\alpha$  treatment.  
675

676 **Figure 4.** Changes in intracellular ROS levels in response to RSV and metabolites at 4 h (A)  
677 and 24 h (B), expressed as percentage towards untreated cells without TNF- $\alpha$  addition. Data  
678 are expressed as mean  $\pm$  SEM of three measurements in triplicates, in three independent  
679 experiments. \* and \*\* indicate significant differences ( $p<0.05$  and  $p<0.001$ , respectively)  
680 compared to the respective control sample without RSV treatment; and # and ## indicate  
681 significant differences ( $p<0.05$  and  $p<0.001$ , respectively) compared to the respective control  
682 sample without TNF- $\alpha$  treatment.  
683

684 **Figure 5.** Secretion of proinflammatory chemokines and vascular endothelial growth factor  
685 after 4 h (T4) and 24 h (T24) exposure to RSV in the co-culture, expressed as percentage  
686 towards untreated cells without TNF- $\alpha$  addition. A) IL-8; B) VEGF; C) ICAM-1. Data  
687 represent the mean  $\pm$  SEM, three measurements in triplicates, in three independent  
688 experiments. \* and \*\* indicate significant differences ( $p<0.05$  and  $p<0.001$ , respectively)  
689 compared to the respective control sample without RSV treatment; and # and ## indicate  
690 significant differences ( $p<0.05$  and  $p<0.001$ , respectively) compared to the respective control  
691 sample without TNF- $\alpha$  treatment.

692

- 1
- 2
- 3
- 4
- 5
- 6
- 7
- 8
- 9
- 10
- 11
- 12
- 13
- 14
- 15
- 16
- 17
- 18
- 19
- 20
- 21
- 22
- 23
- 24
- 25
- 26
- 27
- 28
- 29
- 30
- 31
- 32
- 33
- 34
- 35
- 36
- 37
- 38
- 39
- 40
- 41
- 42
- 43
- 44
- 45
- 46
- 47
- 48
- 49
- 50
- 51
- 52
- 53
- 54
- 55
- 56
- 57
- 58
- 59
- 60
- 61
- 62
- 63
- 64
- 65

693

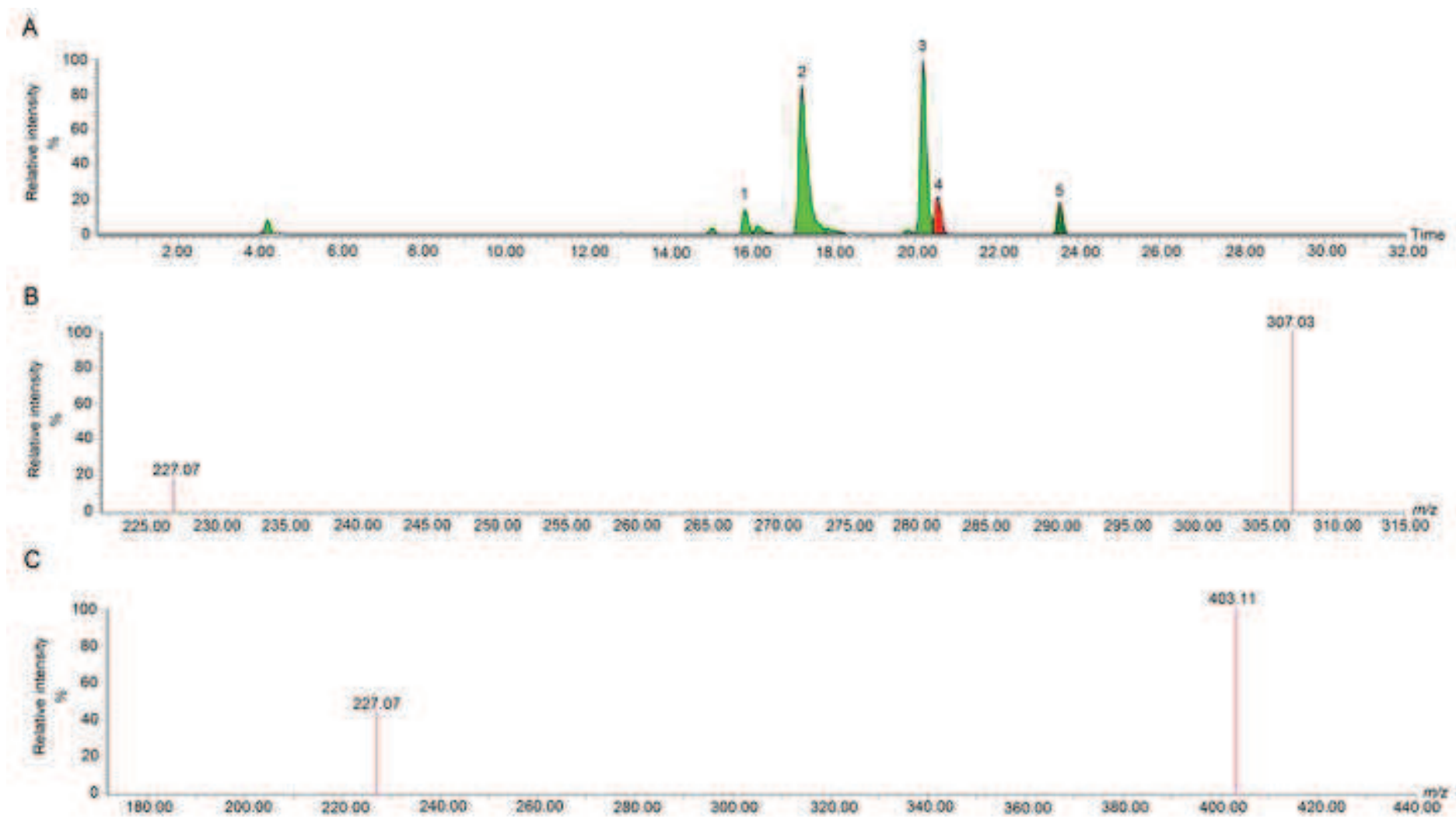
694

**Table 1.** Modifications of RSV and metabolites identified by UPLC-ESI-HDMS/MS<sup>2</sup> after metabolism and transport by Caco-2 cells.

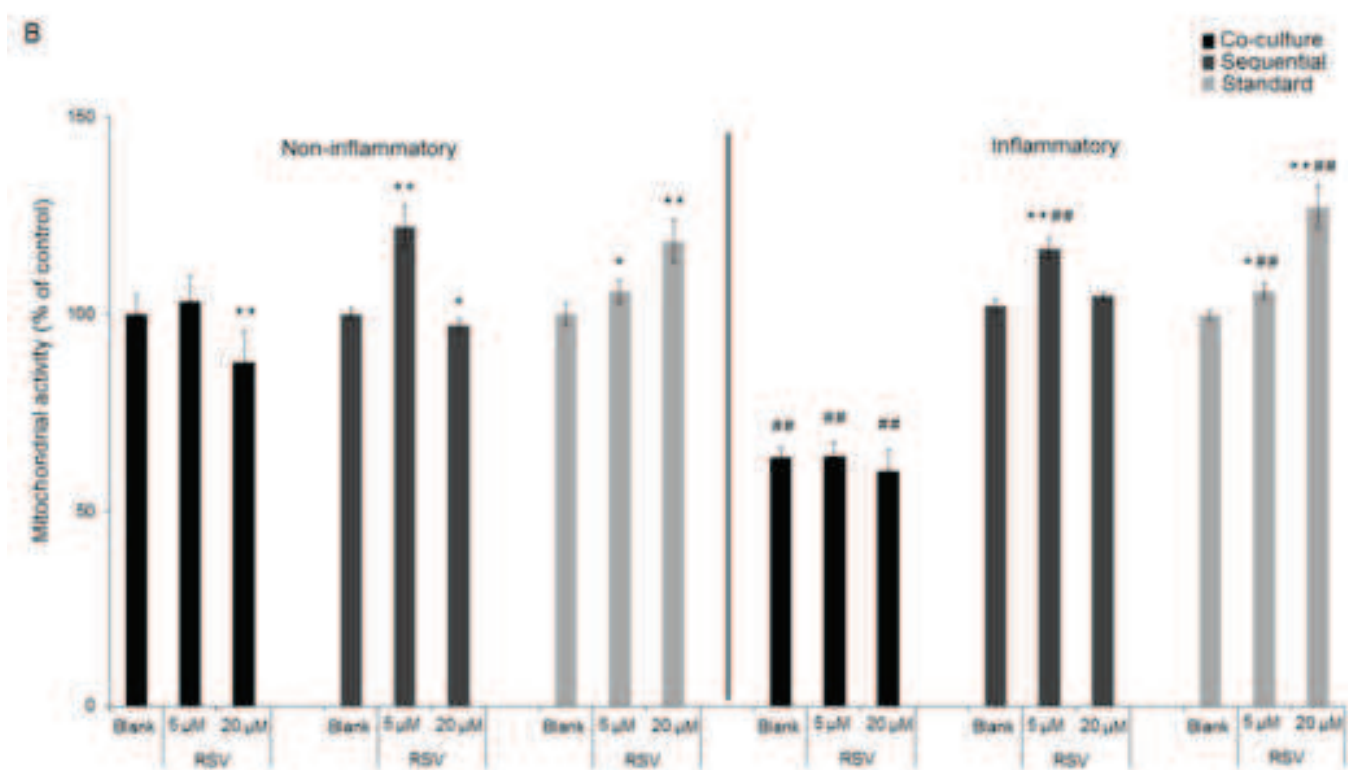
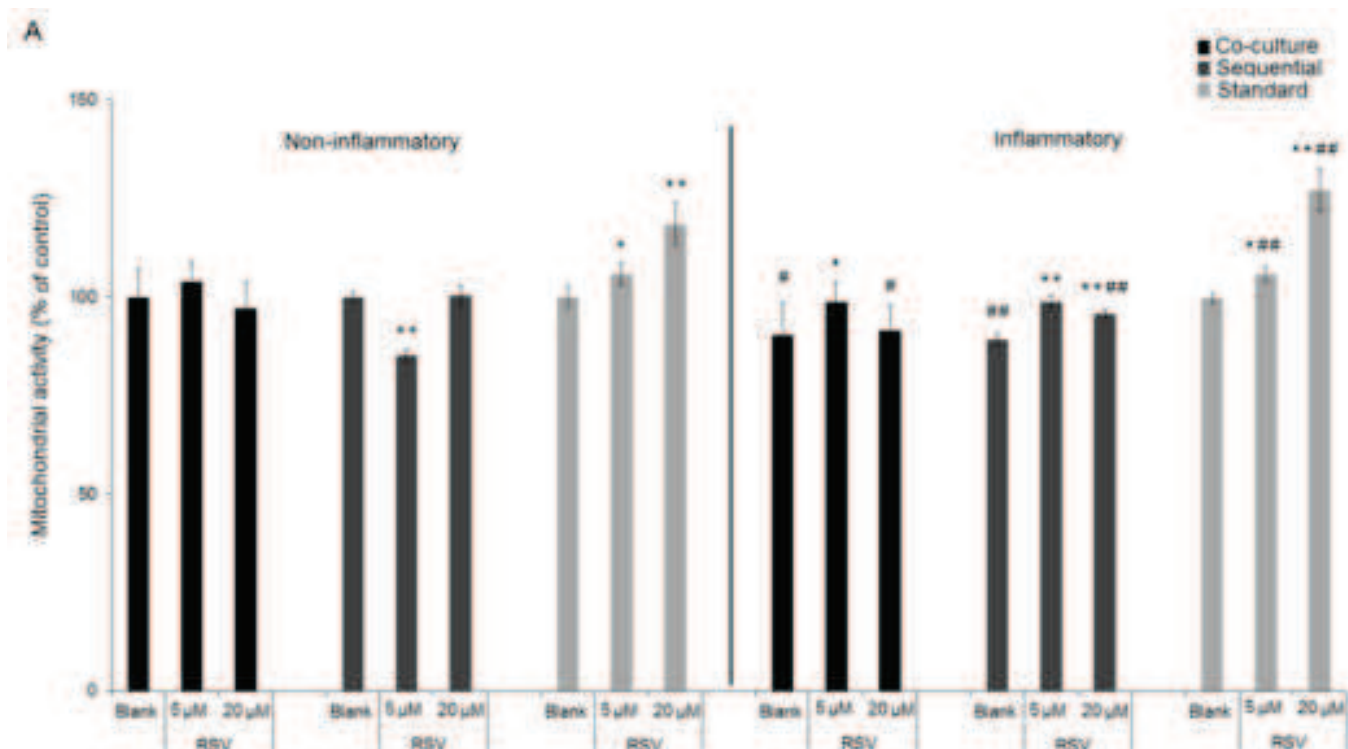
Identified compound	Molecular formula	Rt (min)	Molecular mass	Detected <i>m/z</i>	MS/MS fragment	Neutral loss	Modification
(1) <i>Trans</i> -Resveratrol-4'- <i>O</i> - $\beta$ -glucuronide	C <sub>20</sub> H <sub>20</sub> O <sub>9</sub>	15.85	404.11	403.11	227.07	176	Glucuronide conjugation
(2) <i>Trans</i> -Resveratrol-4'-sulfate	C <sub>14</sub> H <sub>12</sub> O <sub>6</sub> S	17.23	308.04	307.03	227.07	80	Sulfate conjugation
(3) <i>Trans</i> -Resveratrol-3-sulfate	C <sub>14</sub> H <sub>12</sub> O <sub>6</sub> S	20.19	308.04	307.03	227.07	80	Sulfate conjugation
(4) <i>Trans</i> -Resveratrol-3- <i>O</i> - $\beta$ -glucuronide	C <sub>20</sub> H <sub>20</sub> O <sub>9</sub>	20.58	404.11	403.11	227.07	176	Glucuronide conjugation
(5) <i>Trans</i> -Resveratrol	C <sub>14</sub> H <sub>12</sub> O <sub>3</sub>	23.53	228.07	227.07	-	0	-

Figure(s)

[Click here to download high resolution image](#)

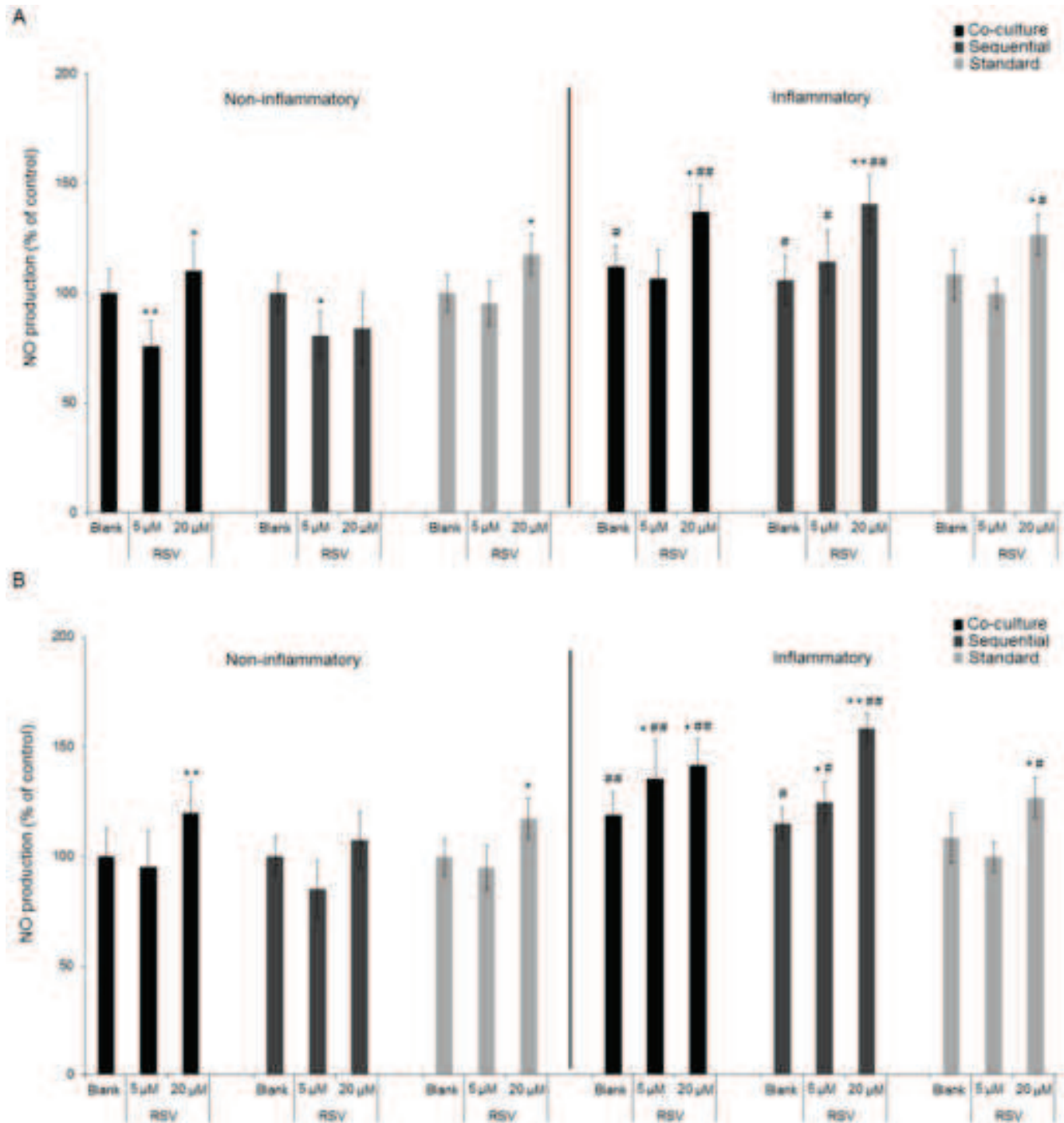


Figure(s)  
[Click here to download high resolution image](#)

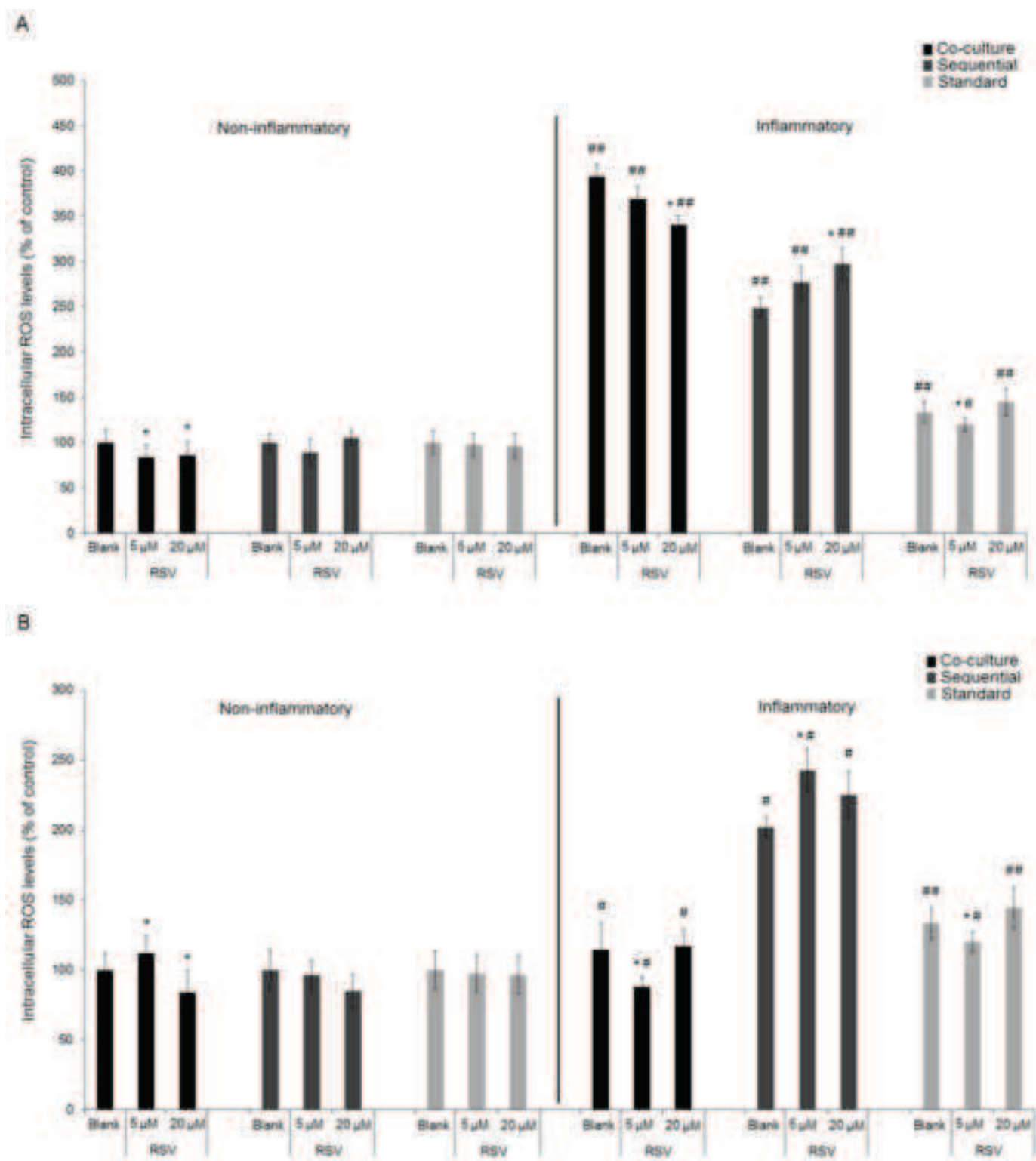




Figure(s)  
[Click here to download high resolution image](#)



Figure(s)  
[Click here to download high resolution image](#)



Figure(s)

[Click here to download high resolution image](#)

